Available online at www.sciencedirect.com
ScienceDirect
Journal of Sound and Vibration 312 (2008) 94–108
JOURNAL OF SOUND AND VIBRATION
www.elsevier.com/locate/jsvi

Effect of ply orientation on the in-plane vibration of single-layer composite plates

Roland L. Woodcock[a,*], Rama B. Bhat[b], Ion G. Stiharu[b]

[a]*United Technologies Research Center, Acoustics Group, Components Department, 411 Silver Lane, MS 129-17, East Hartford, CT 06108, USA*

[b]*Concordia University, Mechanical Engineering, Concave Research Center, 1455 de Maisonneuve Blvd. W., Montreal, Quebec, Canada H3G 1M8*

Received 24 January 2006; received in revised form 28 September 2007; accepted 16 October 2007

Abstract

Composite laminate structures can be designed for specific purposes by optimizing the number of plies and the ply orientations. Previous studies established the behavior of the first natural frequencies of the bending motion of a thin composite plate in the framework of classical plate theory for different boundary conditions. Since plates can also undergo in-plane vibration, the present study is aimed at investigating the effect of the ply orientation on such in-plane vibration. This is made possible through theoretical simulation with a model based on the Rayleigh–Ritz formulation in conjunction with Hamilton principle. The total matrices deduced by minimizing the Hamilton function exhibit a decoupling of bending and membrane motions, which are in plane. The natural frequencies of the membrane motion can therefore be calculated and the ply orientations are investigated for free–free boundary conditions for a square plate. The present model is first validated by comparing the natural frequencies of the bending and in-plane motions of isotropic plates with available data in the literature and the agreement is found to be excellent with the maximum discrepancy being only 0.25%. The validation is then extended to orthotropic plates for the first two bending natural frequencies under simply supported boundary conditions for different ply orientations. The present study establishes that for free–free boundary conditions the first natural frequency of the in-plane vibration of a composite square plate is symmetrical with respect to 45° ply orientation and is maximum for this value. This study suggests that it is possible to use this analysis to design composite plates by properly tailoring ply orientations.

1. Introduction

In many industries, such as Aerospace, Aeronautics, Automotive, the advantage of composite materials over conventional materials has been well established. From a theoretical point of view this has led to the development of numerous models of composite plates for the prediction of different parameters including free vibration. The more common composites used are laminated plates which are typically made of different

*Corresponding author. New address: Hawker Beechcraft Corporation, Acoustics Group, 9709 E. Central, Wichita, KS 67206, USA. Tel.: +1 316 676 7391.

E-mail address: roland_woodcock@hawkerbeechcraft.com (R.L. Woodcock).

0022-460X/$ - see front matter © 2007 Elsevier Ltd. All rights reserved.
doi:10.1016/j.jsv.2007.10.028

Nomenclature

a_{nm} coefficients of W
a, b plate dimensions in x and y directions, respectively
b_{nm}, c_{nm} coefficients of Φ_1 and Φ_2, respectively
B, M_{e1}, M_{e2} subscripts for bending, membranes along x_1 and x_2
$c = \cos(\theta_o), s = \sin(\theta_o)$
d_{nm}, e_{nm} coefficients of φ_1 and φ_2, respectively
e_d density of deformation energy
e_k density of kinetic energy
E_1, E_2 young modulus in x_1 and x_2 directions
G_{12} shear modulus in Ox_1x_2 plane
G_{13}, G_{23} shear modulus in Ox_1x_3 and Ox_2x_3 plane
$\mathscr{H}$ function of Hamilton
K_f, C_f bending translational and rotational stiffness of springs for BC
K_{m1}, K_{m2} membrane translational stiffness per unit length of springs for BC
K_{s1}, K_{s2} shear stiffness per unit length of springs for BC
$[K_{nmpq}]$ stiffness matrix
M_{e1}/M_{e2} subscripts for coupling between membrane in x_1 and x_2 directions
$[M_{nmpq}]$ mass matrix
n, m indices in x_1 and x_2 directions
Q_{ij} reduced stiffness
S area of the plate
S_{e1}/S_{e2} subscripts for coupling between shear in x_1 and x_2 directions
t_1, t_2 two arbitrary times
T kinetic energy
V deformation energy
W transverse displacement
x_1, x_2, x_3 three coordinate axes of the plate
ε_{ij} deformations
Φ_1, Φ_2 membrane motions in x_1 and x_2 directions
φ_1, φ_2 shear motions in x_1 and x_2 directions
ν_1, ν_2 Poisson ratio
θ_o anisotropy angle
σ_{ij} stresses
ρ density of the plate
$\Psi_n(x_1), \Psi_m(x_2)$ admissible functions for the basis

layers bonded together. Basically, each layer is generally orthotropic and has a different orientation of the fibers. The main advantage of composite structures is their ability to be designed for specific purposes [1,2] usually with the proper number of plies and the orientation of each ply.

In structural acoustics, recent work in sound transmission through laminated structures [3] has shown that the fundamental frequency is a key parameter. The natural frequencies are sensitive to the orthotropy properties of composite plates and design-tailoring tools may help in controlling this fundamental frequency. The understanding of prediction models facilitates the development of such tools. Previous studies resulted in a good understanding of the behavior of the first natural frequencies of the bending motion of a thin plate [4–6]. To the authors' best knowledge the review of the open literature indicates that in-plane vibration has received little attention. This is probably because in-plane natural frequencies are higher than bending ones and because in most laminates the bending and membrane stretching motions are usually coupled. However, all such investigations considered several layers of the composite laminates in studying their dynamic behavior. Recent studies [7,8,15] proposed an analysis for isotropic plates. In the present study a model of a finite generally orthotropic single laminate including bending, membrane and shear motions is developed for calculating the free vibration using the Rayleigh–Ritz method employing the variational method. Different displacement fields from the classical plate theory (CPT) to generalized shear deformation theory (GSDT) have been used in the literature [9]. It is well established now that CPT models over-estimate natural frequencies as a consequence of neglecting the shear stresses. GSDT provides a more accurate description of the laminates but at the expense of increased CPU time. The Mindlin first shear deformation theory (FSDT) therefore offers an interesting alternative from an engineering point of view to perform design analysis. A discussion of the main different models used to model composites dynamic behavior is presented in a recent paper [10]. This model is adopted in the present work with appropriate correction factors to account for the non-parabolic description of shear stresses. In order to deal with arbitrary boundary conditions varying continuously from soft to hard, artificial springs are used to control the translational and rotational motions along the contour [3,11]. Such a technique has been successfully used in a recent study [12]. The present paper is mainly concerned with free–free boundary conditions for the composite plate although the validation is

extended to the case of simply supported boundary conditions with varying ply orientation. The equations derived from minimizing the function of Hamilton with respect to the coefficients in the basis lead to the classical equations of motion in terms of mass and stiffness matrices. The formalism adopted in the present modeling allows the contribution of the plate and of the boundary conditions to be superposed [3]. It is shown that the sub-matrices of the bending motion and of the in-plane motions can be separated. It is found that, in accordance with symmetrical laminate models, there is no coupling between bending and membrane motion [9]. This allows the natural frequencies of the membrane motion to be calculated independent of the bending and of the shear motions. Emphasis is placed on the variation of the ply orientations for the membrane motion in both directions including the coupling. The understanding of this phenomenon is important for developing optimization codes of laminate composites.

The present model is first validated by comparing the natural frequencies of the bending motion of isotropic plates. Data are available in the literature for the bending [13] and the membrane [15] in terms of non-dimensional natural frequencies. The convergence of the present formulation is studied and allows the natural frequencies to be accurately calculated by increasing the number of terms accounted for in the different expansions. Excellent agreement is found in the case of a square plate: the maximum discrepancy is 0.25% for the bending and 0.02% for the membrane. The validation is then extended to the case of orthotropic composite Kevlar–Epoxy material. The first two natural frequencies are compared with existing data in the literature [16] for different ply orientations using a finite element formulation. When comparing both results two observations can be made: (1) Results from Ref. [16] are slightly higher (0.3–4%) than those of the present model, this difference being minimum for 45° orientation. The fundamental frequency computed using the present model agrees with the closed-form expression provided in Ref. [1]. (2) Both results are highlighting the same pattern: the natural frequencies are increasing while increasing ply orientations. These results are for the case of simply supported BC where the plate is elastically restrained against translation at the edges (transverse and stretching) and consequently the stiffness of the plate is increased when increasing the orthotropy angle. The model is further used to take advantage of the decoupling of bending and membrane motions.

It is found that bending and membrane motions have different behaviors. For free–free BC the first natural frequency of the membrane reaches a maximum for a 45° orientation while the bending fundamental frequency reaches a minimum. These frequencies are both symmetrical with respect to this orientation. Calculation of the next seven frequencies has been carried out for the membrane motion. They exhibit different behavior, but still remain symmetrical with respect to the 45° orientation.

This study suggests that tools can be developed based on this analysis, which will allow designing composite plates by properly tailoring the ply orientation for specific applications, particularly in sound transmission in structural acoustics.

The rest of the paper is split into two main parts: in the first part the analytical modeling is presented and the second part deals with the numerical simulations and a discussion of the main results.

2. Analytical modeling

2.1. Plate modeling

A baffled finite plate is inserted in a rigid baffle. The geometry of the plate is depicted in Fig. 1. The plate is generally orthotropic and the angle θ_0 is used to describe the orientation of the orthotropic properties with respect to the natural axes of the plate. The displacement field describing the behavior of the plate is the one given by Mindlin model including the in-plane and the bending motions:

$$u_1 = \Phi_1 - x_3 \frac{\partial W}{\partial x_1} - x_3 \varphi_1, \quad u_2 = \Phi_2 - x_3 \frac{\partial W}{\partial x_2} - x_3 \varphi_2, \quad u_3 = W, \tag{1}$$

where the first term of u_1 and of u_2 describes the bending motion of the plate. The five quantities Φ_1, Φ_2, φ_1, φ_2 and W are functions of x_1 and x_2. This displacement field is sketched in Fig. 2.

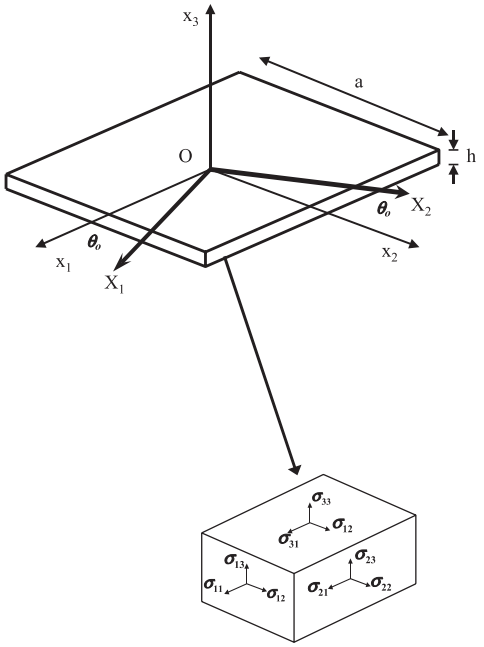

Fig. 1. Sketch illustrating the geometry of the anisotropic composite plate.

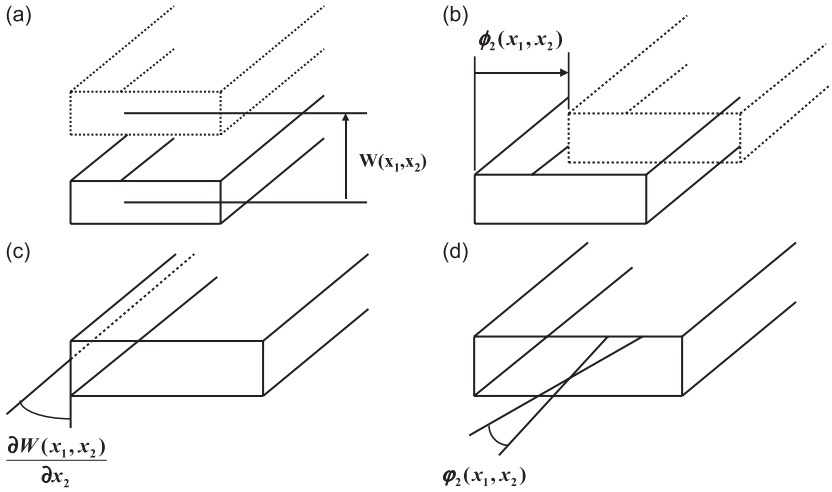

Fig. 2. Sketch illustrating the displacement field: (a) transverse displacement; (b) membrane; (c) flexion; and (d) shear.

The present work deals with the modeling of generally orthotropic plates. The constitutive equations are expressed by the following relations:

$$\begin{pmatrix} \sigma_{11} \\ \sigma_{22} \\ \sigma_{12} \end{pmatrix} = \begin{pmatrix} Q_{11} & Q_{12} & Q_{16} \\ Q_{12} & Q_{22} & Q_{26} \\ Q_{16} & Q_{26} & Q_{66} \end{pmatrix} \begin{pmatrix} \varepsilon_{11} \\ \varepsilon_{22} \\ 2\varepsilon_{12} \end{pmatrix}, \tag{2}$$

$$\begin{pmatrix} \sigma_{23} \\ \sigma_{13} \end{pmatrix} = \begin{pmatrix} Q_{44} & Q_{45} \\ Q_{45} & Q_{55} \end{pmatrix} \begin{pmatrix} 2\varepsilon_{23} \\ 2\varepsilon_{13} \end{pmatrix}, \tag{3}$$

where the Q_{ij} account for the angle of orthotropy in the plane Ox_1x_2. They are given by

$$\begin{pmatrix} Q_{11} \\ Q_{22} \\ Q_{12} \\ Q_{66} \\ Q_{16} \\ Q_{26} \end{pmatrix} = \begin{pmatrix} c^4 & s^4 & 2s^2c^2 & 4c^2s^2 \\ s^4 & c^4 & 2s^2c^2 & 4c^2s^2 \\ c^2s^2 & c^2s^2 & c^4+s^4 & -4s^2c^2 \\ s^2c^2 & s^2c^2 & -2s^2c^2 & (c^2-s^2)^2 \\ c^3s & -s^3c & s^3c-sc^3 & 2sc(s^2-c^2) \\ s^3c & -sc^3 & c^3s-s^3c & 2sc(c^2-s^2) \end{pmatrix} \begin{pmatrix} \overline{Q_{11}} \\ \overline{Q_{22}} \\ \overline{Q_{12}} \\ \overline{Q_{66}} \end{pmatrix}, \tag{4}$$

with Q_{16} and Q_{26} being non-zero to account for the general orthotropy. The $\overline{Q_{ij}}$ are related to the engineering parameters by

$$\overline{Q_{11}} = \frac{E_1}{1-\nu_1\nu_2}, \quad \overline{Q_{12}} = \frac{\nu_1 E_2}{1-\nu_1\nu_2} = \frac{\nu_2 E_1}{1-\nu_1\nu_2}, \quad \overline{Q_{22}} = \frac{E_2}{1-\nu_1\nu_2}, \quad \overline{Q_{66}} = G_{12}, \tag{5}$$

$$\overline{Q_{44}} = G_{23}, \quad \overline{Q_{55}} = G_{13}, \tag{6}$$

where E_1, E_2, ν_1, ν_2 and G_{12} are the five parameters which fully characterize the plate in the Ox_1x_2 plane. The strain field is related to the displacement field:

$$\varepsilon_{ij} = \frac{1}{2}\left(\frac{\partial u_i}{\partial x_j} + \frac{\partial u_j}{\partial x_i}\right), \quad i,j = 1,2. \tag{7}$$

The function of Hamilton $\mathscr{H}$ can therefore be built as a function of the kinetic energy T and the deformation energy V. This functional is calculated as an integral between two arbitrary times t_1 and t_2:

$$\mathscr{H} = \int_{t_1}^{t_2} \mathrm{d}t, \quad \int_S (T-V)\,\mathrm{d}S, \tag{8}$$

where the integral performed over the surface of the plate represents the energy of the system. The density of kinetic and deformation energies are first calculated in order to perform the calculation of T and V. The density of kinetic energy over the surface of the plate is given by

$$e_k = \frac{1}{2}\int_{-h/2}^{h/2} \rho \sum_i u_i^2 \,\mathrm{d}x_3. \tag{9}$$

The following equation is straightforward after a few algebraic calculations:

$$e_k = \frac{1}{2}\left\{ \delta_1\left(\frac{\partial^2 W}{\partial x_1 \partial t}\right)^2 + \delta_2\left(\frac{\partial \varphi_1}{\partial t}\right)^2 + \delta_3\left(\frac{\partial \Phi_1}{\partial t}\right)^2 + \delta_4\left(\frac{\partial^2 W}{\partial x_1 \partial t}\frac{\varphi_1}{\partial t}\right) + \delta_7\left(\frac{\partial^2 W}{\partial x_2 \partial t}\right)^2 + \delta_8\left(\frac{\partial \varphi_2}{\partial t}\right)^2 + \delta_9\left(\frac{\partial \Phi_2}{\partial t}\right)^2 + \delta_{10}\left(\frac{\partial^2 W}{\partial x_2 \partial t}\frac{\partial \varphi_2}{\partial t}\right) + \delta_{13}\left(\frac{\partial W}{\partial t}\right)^2 \right\},$$

The δ_i parameters have been used in order to have concise expressions for e_k and to allow the comparison with a more general model [17] previously developed for which the present formulation can be viewed as a special case. The δ_i are functions of the density and of the thickness of the plate and are defined as

$$\delta_1 = \delta_2 = \delta_7 = \delta_8 = \rho\frac{h^3}{12}, \quad \delta_3 = \delta_9 = \delta_{13} = \rho h, \quad \delta_4 = \delta_{10} = 2\rho\frac{h^3}{12}. \tag{10}$$

The density of the deformation energy is given by

$$e_d = \frac{1}{2}\int_{-h/2}^{h/2} \sigma_{ij}\,\varepsilon_{ij}\,\mathrm{d}x_3. \tag{11}$$

The calculation of e_d is straightforward and leads to the following expression:

$$
\begin{aligned}
e_d = \frac{1}{2}\Bigg\{ & \lambda_1\left(\frac{\partial^2 W}{\partial x_1^2}\right)^2 + \lambda_2\left(\frac{\partial \varphi_1}{\partial x_1}\right)^2 + \lambda_3\left(\frac{\partial \Phi_1}{\partial x_1}\right)^2 + \lambda_4\left(\frac{\partial^2 W}{\partial x_1^2}\frac{\partial \varphi_1}{\partial x_1}\right)^2 + \lambda_7\left(\frac{\partial^2 W}{\partial x_2^2}\right)^2 \\
& + \lambda_8\left(\frac{\partial \varphi_2}{\partial x_2}\right)^2 + \lambda_9\left(\frac{\partial \Phi_2}{\partial x_2}\right)^2 + \lambda_{10}\left(\frac{\partial^2 W}{\partial x_2^2}\frac{\partial \varphi_2}{\partial x_2}\right)^2 + \lambda_{13}\left(\frac{\partial^2 W}{\partial x_1^2}\frac{\partial^2 W}{\partial x_2^2}\right) \\
& + \lambda_{14}\left(\frac{\partial^2 W}{\partial x_1^2}\frac{\partial \varphi_2}{\partial x_2}\right) + \lambda_{16}\left(\frac{\partial^2 W}{\partial x_2^2}\frac{\partial \varphi_1}{\partial x_1}\right) + \lambda_{17}\left(\frac{\partial \varphi_2}{\partial x_2}\frac{\partial \varphi_2}{\partial x_2}\right) + \lambda_{21}\left(\frac{\partial \Phi_1}{\partial x_1}\frac{\partial \Phi_2}{\partial x_2}\right) \\
& + \lambda_{22}\left(\frac{\partial^2 W}{\partial x_1 \partial x_2}\right)^2 + \lambda_{23}\left(\frac{\partial \varphi_1}{\partial x_2}\right)^2 + \lambda_{24}\left(\frac{\partial \varphi_2}{\partial x_1}\right)^2 + \lambda_{25}\left(\frac{\partial \Phi_1}{\partial x_2}\right)^2 \\
& + \lambda_{26}\left(\frac{\partial \Phi_2}{\partial x_1}\right)^2 + \lambda_{27}\left(\frac{\partial^2 W}{\partial x_1 \partial x_2}\frac{\partial \varphi_1}{\partial x_2}\right) + \lambda_{28}\left(\frac{\partial^2 W}{\partial x_1 \partial x_2}\frac{\partial \varphi_2}{\partial x_1}\right) + \lambda_{31}\left(\frac{\partial \varphi_1}{\partial x_2}\frac{\partial \varphi_2}{\partial x_1}\right) \\
& + \lambda_{36}\left(\frac{\partial \Phi_1}{\partial x_2}\frac{\partial \Phi_2}{\partial x_1}\right) + \lambda_{37}\varphi_1^2 + \lambda_{38}\varphi_2^2 + \lambda_{39}\left(\frac{\partial^2 W}{\partial x_1^2}\frac{\partial^2 W}{\partial x_1 \partial x_2}\right) \\
& + \lambda_{40}\left(\frac{\partial^2 W}{\partial x_1^2}\frac{\partial \varphi_1}{\partial x_2}\right) + \lambda_{42}\left(\frac{\partial^2 W}{\partial x_1 \partial x_2}\frac{\partial \varphi_1}{\partial x_1}\right) + \lambda_{43}\left(\frac{\partial \varphi_1}{\partial x_1}\frac{\partial \varphi_1}{\partial x_2}\right) + \lambda_{47}\left(\frac{\partial^2 \Phi_1}{\partial x_1 \partial x_2}\right) \\
& + \lambda_{48}\left(\frac{\partial^2 W}{\partial x_1^2}\frac{\partial \varphi_2}{\partial x_1}\right) + \lambda_{50}\left(\frac{\partial \varphi_1}{\partial x_1}\frac{\partial \varphi_2}{\partial x_1}\right) + \lambda_{53}\left(\frac{\partial \Phi_1}{\partial x_1}\frac{\partial \Phi_2}{\partial x_2}\right) + \lambda_{54}\left(\frac{\partial^2 W}{\partial x_2^2}\frac{\partial^2 W}{\partial x_1 \partial x_2}\right) \\
& + \lambda_{55}\left(\frac{\partial^2 W}{\partial x_2^2}\frac{\partial \varphi_1}{\partial x_2}\right) + \lambda_{57}\left(\frac{\partial^2 W}{\partial x_1 \partial x_2}\frac{\partial \varphi_2}{\partial x_2}\right) + \lambda_{58}\left(\frac{\partial \varphi_1}{\partial x_2}\frac{\partial \varphi_2}{\partial x_2}\right) + \lambda_{62}\left(\frac{\partial \Phi_1}{\partial x_2}\frac{\partial \Phi_2}{\partial x_2}\right) \\
& + \lambda_{63}\left(\frac{\partial^2 W}{\partial x_2^2}\frac{\partial \varphi_2}{\partial x_1}\right) + \lambda_{65}\left(\frac{\partial \varphi_2}{\partial x_1}\frac{\partial \varphi_2}{\partial x_2}\right) + \lambda_{68}\left(\frac{\partial^2 \Phi_2}{\partial x_1 \partial x_2}\right) + \lambda_{69}\varphi_1\varphi_2 \Bigg\},
\end{aligned}
$$

with

$$
\begin{aligned}
& \lambda_1 = Q_{11}\frac{h^3}{12}, \quad \lambda_2 = Q_{11}\frac{h^3}{12}, \quad \lambda_3 = Q_{11}h, \\
& \lambda_4 = 2Q_{11}\frac{h^3}{12}, \quad \lambda_7 = Q_{22}\frac{h^3}{12}, \quad \lambda_8 = Q_{22}\frac{h^3}{12}, \\
& \lambda_9 = Q_{22}h, \quad \lambda_{10} = 2Q_{22}\frac{h^3}{12}, \quad \lambda_{13} = 2Q_{12}\frac{h^3}{12}, \\
& \lambda_{14} = 2Q_{12}\frac{h^3}{12}, \quad \lambda_{16} = 2Q_{12}\frac{h^3}{12}, \quad \lambda_{17} = 2Q_{12}\frac{h^3}{12}, \\
& \lambda_{21} = 2Q_{12}h, \quad \lambda_{22} = 4Q_{66}\frac{h^3}{12}, \quad \lambda_{23} = Q_{66}\frac{h^3}{12}, \\
& \lambda_{24} = Q_{66}\frac{h^3}{12}, \quad \lambda_{25} = Q_{66}h, \quad \lambda_{26} = Q_{66}h \\
& \lambda_{27} = 4Q_{66}\frac{h^3}{12}, \quad \lambda_{28} = 4Q_{66}\frac{h^3}{12}, \quad \lambda_{31} = 2Q_{66}\frac{h^3}{12}, \\
& \lambda_{36} = 2Q_{66}h, \quad \lambda_{37} = Q_{55}h, \quad \lambda_{38} = Q_{44}h, \\
& \lambda_{39} = 4Q_{16}\frac{h^3}{12}, \quad \lambda_{40} = 2Q_{16}\frac{h^3}{12}, \quad \lambda_{42} = 4Q_{16}\frac{h^3}{12}, \\
& \lambda_{43} = 2Q_{16}\frac{h^3}{12}, \quad \lambda_{47} = 2Q_{16}h, \quad \lambda_{48} = 2Q_{16}\frac{h^3}{12},
\end{aligned}
$$

$$\lambda_{50} = 2Q_{16}\frac{h^3}{12}, \quad \lambda_{53} = 2Q_{16}h, \quad \lambda_{54} = 4Q_{26}\frac{h^3}{12},$$
$$\lambda_{55} = 2Q_{26}\frac{h^3}{12}, \quad \lambda_{57} = 4Q_{26}\frac{h^3}{12}, \quad \lambda_{58} = 2Q_{26}\frac{h^3}{12},$$
$$\lambda_{62} = 2Q_{26}h, \quad \lambda_{63} = 2Q_{26}\frac{h^3}{12}, \quad \lambda_{65} = 2Q_{26}\frac{h^3}{12},$$
$$\lambda_{68} = 2Q_{26}h, \quad \lambda_{69} = 2Q_{45}h.$$

In order to use the variational principles and the Rayleigh–Ritz method, admissible functions $\Psi_n(x_1)$ and $\Psi_m(x_2)$ are adopted for the transverse displacement, the membrane motions and the shear motions:

$$W(x_1, x_2) = \sum_n \sum_m a_{nm}\Psi_n(x_1)\Psi_m(x_2), \tag{12}$$

$$\Phi_1(x_1, x_2) = \sum_n \sum_m b_{nm}\Psi_n(x_1)\Psi_m(x_2), \tag{13}$$

$$\Phi_2(x_1, x_2) = \sum_n \sum_m c_{nm}\Psi_n(x_1)\Psi_m(x_2), \tag{14}$$

$$\varphi_1(x_1, x_2) = \sum_n \sum_m d_{nm}\Psi_n(x_1)\Psi_m(x_2), \tag{15}$$

$$\varphi_2(x_1, x_2) = \sum_n \sum_m e_{nm}\Psi_n(x_1)\Psi_m(x_2), \tag{16}$$

where a_{nm}, b_{nm}, c_{nm}, d_{nm} and e_{nm} are arbitrary coefficients to be determined. Following Berry et al. [11] and Woodcock and Nicolas [3] simple polynomial functions are chosen for $\Psi(x)$ as

$$\Psi_n(x_1) = \left(\frac{2}{a}x_1\right)^n, \quad \Psi_m(x_2) = \left(\frac{2}{b}x_2\right)^m. \tag{17}$$

These functions in conjunction with artificial springs along the contour to control the translational and rotational motion will allow arbitrary boundary conditions to be modeled.

The function of Hamilton $\mathscr{H}$ is then a function of the different unknowns. Minimizing $\mathscr{H}$ with respect to the unknowns leads to the classical equation of motion accounting for the mass and stiffness matrix defined as

$$[M^{\text{Plate}}_{nmpq}] = \begin{bmatrix} [M^{B}_{nmpq}] & [0] & [0] & [M^{B/S_{e1}}_{nmpq}] & [M^{B/S_{e2}}_{nmpq}] \\ [0] & [M^{Me_1}_{nmpq}] & [0] & [0] & [0] \\ [0] & [0] & [M^{Me_2}_{nmpq}] & [0] & [0] \\ [M^{S_{e1}/B}_{nmpq}] & [0] & [0] & [M^{S_{e1}}_{nmpq}] & [0] \\ [M^{S_{e2}/B}_{nmpq}] & [0] & [0] & [0] & [M^{S_{e2}}_{nmpq}] \end{bmatrix}, \tag{18}$$

$$[M^{B}_{nmpq}] = [\delta_1 M_1 + \delta_7 M_2 + \delta_{13} M_3], \tag{19}$$

$$[M^{M_{e1}}_{nmpq}] = [\delta_3 M_3]; \quad [M^{M_{e2}}_{nmpq}] = [\delta_9 M_3], \tag{20}$$

$$[M^{S_{e1}}_{nmpq}] = [\delta_2 M_3]; \quad [M^{S_{e2}}_{nmpq}] = [\delta_8 M_3], \tag{21}$$

$$[M^{B/S_{e1}}_{nmpq}] = \tfrac{1}{2}[\delta_4 M_4]; \quad [M^{B/S_{e2}}_{nmpq}] = \tfrac{1}{2}[\delta_{10} M_5], \tag{22}$$

$$[K^{\text{Plate}}_{nmpq}] = \begin{bmatrix} [K^{B}_{nmpq}] & [0] & [0] & [K^{B/S_{e1}}_{nmpq}] & [K^{B/S_{e2}}_{nmpq}] \\ [0] & [K^{M_{e1}}_{nmpq}] & [K^{Me_1/Me_2}_{nmpq}] & [0] & [0] \\ [0] & [K^{Me_2/Me_1}_{nmpq}] & [K^{M_{e2}}_{nmpq}] & [0] & [0] \\ [K^{S_{e1}/B}_{nmpq}] & [0] & [0] & [K^{S_{e1}}_{nmpq}] & [K^{S_{e1}/S_{e2}}_{nmpq}] \\ [K^{S_{e2}/B}_{nmpq}] & [0] & [0] & [K^{S_{e2}/S_{e1}}_{nmpq}] & [K^{S_{e2}}_{nmpq}] \end{bmatrix}, \tag{23}$$

The mass and stiffness show that there is no coupling between bending and membrane motions and between membrane and shearing. The elements of the sub-matrices are given by

$$[K^{B}_{nmpq}] = \tfrac{1}{2}[2\lambda_1 K_1 + 2\lambda_7 K_2 + \lambda_{13} K_{21} + 2\lambda_{22} K_4 + \lambda_{39} K_{22} + \lambda_{54} K_{23}], \tag{24}$$

$$[K^{M_{e1}}_{nmpq}] = \tfrac{1}{2}[2\lambda_3 K_{11} + 2\lambda_{25} K_{12} + \lambda_{47} K_{24}], \tag{25}$$

$$[K^{M_{e2}}_{nmpq}] = \tfrac{1}{2}[2\lambda_9 K_{12} + 2\lambda_{26} K_{11} + \lambda_{68} K_{24}], \tag{26}$$

$$[K^{M_{e1}/M_{e2}}_{nmpq}] = \tfrac{1}{2}[\lambda_{21} K_{13} + \lambda_{36} K_{14} + \lambda_{53} K_{11} + \lambda_{62} K_{12}], \tag{27}$$

$$[K^{S_{e1}}_{nmpq}] = \tfrac{1}{2}[2\lambda_2 K_{11} + 2\lambda_{23} K_{12} + \lambda_{43} K_{24} + 2\lambda_{37} K_{15}], \tag{28}$$

$$[K^{S_{e2}}_{nmpq}] = \tfrac{1}{2}[2\lambda_8 K_{12} + 2\lambda_{24} K_{11} + \lambda_{65} K_{24} + 2\lambda_{38} K_{15}], \tag{29}$$

$$[K^{S_{e1}/S_{e2}}_{nmpq}] = \tfrac{1}{2}[\lambda_{17} K_{13} + \lambda_{31} K_{14} + \lambda_{50} K_{11} + \lambda_{58} K_{12} + \lambda_{69} K_{15}], \tag{30}$$

$$[K^{B/S_{e1}}_{nmpq}] = \tfrac{1}{2}[\lambda_4 K_5 + \lambda_{16} K_6 + \lambda_{27} K_7 + \lambda_{40} K_9 + \lambda_{42} K_{10} + \lambda_{55} K_8], \tag{31}$$

$$[K^{B/S_{e2}}_{nmpq}] = \tfrac{1}{2}[\lambda_{10} K_8 + \lambda_{14} K_9 + \lambda_{28} K_{10} + \lambda_{48} K_5 + \lambda_{57} K_7 + \lambda_{63} K_6], \tag{32}$$

The preceding equations M_i and K_i are given in the Appendix. The eqns assume the following vector of unknowns:

$$V_u = \{[a_{nm}], [b_{nm}], [c_{nm}], [d_{nm}], [e_{nm}]\}^{\mathrm{T}}. \tag{33}$$

2.2. On the boundary conditions modeling

In order to deal with the different cases encountered in real situations, boundary conditions must be accounted for. This is achieved by the means of six artificial springs to model the dynamic behavior at the boundaries: two for the bending motion to control the translational and rotational motions, two for the membrane (in both directions) and finally two for the shear motion (both directions) as well. Appropriate values of the stiffnesses of these springs allow the different configurations to be modeled. The case of free–free boundary conditions is modeled by setting values of zero to the six springs. The modeling was proposed in Ref. [17] for the general case of stratified structures and the principle for thin plate was illustrated for example in Ref. [3].

$$e_p = \frac{1}{2}\int_{-h_n/2}^{h_n/2} \left[k_f W^2 + c_f \left(\frac{\partial W}{\partial n}\right)^2 + k_{m1}(\phi_1)^2 + k_{m2}(\phi_2)^2 + k_{s1}(\varphi_1)^2 + k_{s2}(\varphi_2)^2 \right] \mathrm{d}(R_n - z), \tag{34}$$

Rigidities per unit length are defined so that e_p is expressed as follows:

$$e_p = \frac{1}{2}\left\{ K_f W^2 + C_f \left(\frac{\partial W}{\partial n}\right)^2 + K_{m1}(\phi_1)^2 + K_{m2}(\phi_2)^2 + K_{s1}(\varphi_1)^2 + K_{s2}(\varphi_2)^2 \right\}. \tag{35}$$

The function of Hamilton of the BC is defined as

$$\mathscr{H}^{bc} = \int_{t_0}^{t_1} \int_{\Gamma} (-e_p)\, \mathrm{d}\,\Gamma\, \mathrm{d}t. \tag{36}$$

The integral on the contour Γ is split into four in order to account for the individual contributions of the four edges of the plate. This allows the simulation of different BC on each edge.

3. Numerical analysis

The accuracy of the natural frequencies depends on the number of terms used in the series in Eqs. (12)–(14). In all the results presented hereafter, the convergence of the series has been carefully studied. The number of terms is progressively increased. In the present paper, simulations are undertaken on a square plate with a dimension $a = 0.376\,\mathrm{m}$. The properties of the plate are given in Table 1.

3.1. Validation of the proposed model

The present modeling is validated on a square aluminum isotropic plate and on an orthotropic plate (Kevlar–Epoxy material, Material III of Table 1 with a dimension $a = 0.3048\,\mathrm{m}$ and a thickness of 1.077 mm). Natural non-dimensional frequencies for free–free boundary condition are available in the textbook by Gorman [13] for the bending. For the present formulation, natural frequencies were performed using the IMSL routines. The sub-matrix of the bending motion is extracted from the whole matrix, which exhibits no coupling between the bending and the in-plane motions. Results are presented in Table 2 for the isotropic plate. The thickness of the plate is 3.175 mm. The first row presents natural frequencies deduced from data given in Ref. [13] while the second row indicates natural frequencies obtained with the present formulation. The values in brackets represent the number of terms which ensures the convergence of the series in the present modeling. This table shows that the agreement is excellent; the maximum discrepancy observed is 0.25%.

Table 1
Material properties of composite plates

Material	E_1 (Pa)	E_2 (Pa)	G (Pa)	ν_{12}	ρ (kg/m^3)	ν_{21}
Material I	13.8×10^6	0.9×10^6	0.71×10^6	0.20	100	0.0195
Material II	20.3×10^{10}	1.12×10^{10}	0.84×10^{10}	0.32	1600	0.01766
Material III	7.6×10^{10}	0.55×10^{10}	0.23×10^{10}	0.34	1600	0.0246

Table 2
Comparison of the bending natural frequencies of a square aluminum isotropic plate

Ref. [14] (Hz)	Present model (Hz)
69.94	70.12 ($N = 12$)
102.11	102.26 ($N = 12$)
129.73	129.62 ($N = 12$)
333.35	333.79 ($N = 12$)
361.82	362.32 ($N = 12$)
408.77	408.80 ($N = 12$)
618.46	618.29 ($N = 15$)
650.54	650.15 ($N = 15$)
803.30	803.70 ($N = 15$)
849.19	849.54 ($N = 15$)
1075.88	1075.58 ($N = 17$)

The validation is then extended to the case of orthotropic composite Kevlar–Epoxy material. The first two natural frequencies are compared with existing data in the literature [16] for different ply orientations using a finite element formulation and the results are presented in Tables 4 and 5 When comparing both results two observations can be made: (1) Results from Ref. [16] are slightly higher (0.3–4%) than those of the present model, this difference being minimum for 45° orientation. The fundamental frequency computed using the present model agrees with the closed-form expression provided in Ref. [1]. (2) Both results are highlighting the same pattern: the natural frequencies are increasing while increasing ply orientations. These results are for the case of simply supported BC, the displacement at the edges (transverse and stretching) are zero and consequently the stiffness of the plate is increased when increasing the orthotropy angle and is uniformly distributed in its area resulting in an increase of the natural frequencies.

Results for the case of in-plane vibration are compared with those given in Ref. [15], which provide the six natural frequencies of a square plate for the membrane motion. The result of the comparison is presented in Table 3. The value of 9 in brackets represents the number of terms which ensures the convergence of the series. Once again the agreement is excellent, the maximum discrepancy obtained is within 0.02%. The validation has been extended to the case of simply-supported boundary conditions for an orthotropic plate. Tables 4 and 5

Table 3
Comparison of the membrane first natural frequencies of an isotropic square plate

Ref. [15] (Hz)	Present model (Hz)
276.346	276.290 ($N = 9$)
294.324	294.280 ($N = 9$)
294.324	294.280 ($N = 9$)
312.898	312.955 ($N = 9$)
355.642	355.692 ($N = 9$)
411.006	411.040 ($N = 9$)

Table 4
Comparison of the fundamental bending frequency of an orthotropic plate under simply-supported boundary conditions—Material III

Angle (deg.)	FEM [16] (Hz)	Present model (Hz)
0	22.07	21.22
15	22.09	21.30
30	22.13	21.71
45	22.14	22.07
60	22.12	21.71
75	22.08	21.30
90	22.06	21.22

Table 5
Comparison of the second natural bending frequency of an orthotropic plate under simply-supported boundary conditions—Material III

Angle (deg.)	FEM [16] (Hz)	Present model (Hz)
0	30.32	32.06
15	33.25	34.52
30	40.48	39.16
45	46.81	41.23
60	40.46	39.16
75	33.25	34.52
90	30.36	32.06

show the results for the fundamental and second natural frequency respectively. The comparison between the present simulations and existing data in the literature exhibits a larger discrepancy. Further work is necessary to investigate this point.

3.2. Effect of the ply orientation on the bending natural frequencies

The fundamental frequency is of primary interest in structural acoustics particularly in sound transmission [3]. The effect of ply orientation under free–free boundary conditions is reported in this section for a composite material whose mechanical properties are listed in Table 1. The behavior of the fundamental frequency is studied versus the ply orientation varying from 0° to 90°. The plate is square with a thickness of 1 mm. Table 6 shows that the frequency decreases with increasing angle, reaching a minimum value for a 45° orientation. This frequency is symmetrical with respect to the 45° orientation. It is interesting to point out that an inverse behavior was reported in the literature [16] for the case of simply supported boundary conditions of a square plate.

3.3. Effect of the ply orientation on the in-plane vibration

As shown in the theoretical calculation, the decoupling of the bending and the membrane motions allows the in-plane vibration to be investigated independent of the bending motion. There is a lack of information in the literature regarding the in-plane vibration mainly for two reasons. Firstly, in most laminates there is a coupling between the different motions and secondly, the membrane natural frequencies are higher than the bending ones for typical plates. In the present paper the in-plane natural frequencies are calculated for a square composite plate whose mechanical properties are listed in Table 1. It has been verified that the membrane natural frequencies are not dependent on the thickness since the in-plane vibration represents the behavior of the plate on its area. From the point of view of geometrical parameters, only the dimensions a and b are of importance.

In Eqs. (18), (23), the membrane in x_1 and x_2 directions has been isolated without and with coupling terms. These sub-matrices are extracted from the whole matrix and IMSL routines are then used to perform the calculation of the natural frequencies. The first column of Table 7 indicates the angle of orthotropy, the three other ones give the natural frequencies of the membrane in x_1 direction, in x_2 direction and in both directions with coupling terms. For design purposes, results were reported in the paper by Bert [2] for the bending motion. It is shown in the present study that the membrane first natural frequencies are symmetrical with respect to 45°: the frequency increases from 0° to 45° and decreases from 45° to 90° as depicted in Table 8. The formulation developed in the present paper allows simulation of a system with a large number of degrees of freedom. Several natural frequencies can therefore be calculated and Table 8 presents results of the next seven frequencies. The symbol *Fi* is used to designate the natural

Table 6
Bending fundamental frequency—Material II

Angle (deg.)	Frequency (Hz)	Angle (deg.)	Frequency (Hz)
0	16.991	50	16.147
5	16.934	55	16.179
10	16.793	60	16.239
15	16.625	65	16.334
20	16.465	70	16.465
25	16.334	75	16.625
30	16.239	80	16.793
35	16.179	85	16.934
40	16.147	90	16.991
45	16.138		

Table 7
First natural frequency of the membrane—Material I

Angle (deg.)	M_{e1} (Hz)	M_{e2} (Hz)	$M_{e1} + M_{e2}$ (Hz)
0	112.051	112.051	109.865
5	112.399	116.997	110.202
10	113.396	122.097	111.190
15	114.922	123.585	112.751
20	116.799	124.522	114.761
25	118.814	125.283	117.027
30	120.753	125.784	119.282
35	122.458	125.908	121.210
40	123.848	125.607	122.511
45	124.905	124.905	122.970
50	125.607	123.848	122.511
55	125.908	122.458	121.210
60	125.784	120.753	119.282
65	125.283	118.814	117.027
70	124.522	116.799	114.761
75	123.585	114.922	112.751
80	122.097	113.396	111.190
85	116.997	112.399	110.202
90	112.051	112.051	109.865

Table 8
Effect of the ply orientation on the membrane natural frequencies—Material I

Angle (deg.)	F_2	F_3	F_4	F_5	F_6	F_7	F_8
0	126.229	138.312	205.001	223.847	225.185	236.265	252.379
5	125.849	139.128	203.911	221.171	223.439	238.117	253.949
10	124.987	141.267	200.753	214.488	219.423	242.530	257.235
15	124.084	144.199	195.728	205.220	215.076	248.727	260.103
20	123.401	147.503	189.131	194.614	211.937	256.342	261.330
25	123.050	150.838	181.785	184.064	210.986	260.262	263.974
30	123.042	153.883	174.740	174.883	212.603	256.321	267.972
35	123.296	156.330	167.440	169.398	216.787	249.473	268.075
40	123.624	157.916	162.741	165.911	223.153	240.905	268.195
45	123.776	158.464	161.108	164.717	229.380	233.837	269.256
50	123.624	157.916	162.741	165.911	223.153	240.905	268.195
55	123.296	156.330	167.440	169.398	216.787	249.473	268.075
60	123.042	153.883	174.740	174.883	212.603	256.321	267.972
65	123.050	150.838	181.785	184.064	210.986	260.262	263.974
70	123.401	147.503	189.131	194.614	211.937	256.342	261.330
75	124.084	144.199	195.728	205.220	215.076	248.727	260.103
80	124.987	141.267	200.753	214.488	219.423	242.530	257.235
85	125.849	139.128	203.911	221.171	223.439	238.117	253.949
90	126.229	138.312	205.001	223.847	225.185	236.265	252.379

frequencies in Hz. All these frequencies are symmetrical with respect to the 45° orientation. The second, fourth, and fifth frequencies decrease with increasing angle while the third and eighth frequencies have an inverse behavior. The sixth and seventh frequencies exhibit either a first minimum or a first maximum for 25° orientation. These results show that all the natural frequencies do not exhibit the same behavior and that this must be accounted for when developing optimization codes according to the frequency range involved.

4. Conclusions

The ply orientation is a key parameter in optimizing composite plates for design purposes. Previous studies reported data on the effect of ply orientations on bending natural frequencies, but very little information on in-plane vibration is available in the literature. The present paper investigated the effect of ply orientation on the in-plane vibration, namely the membrane natural frequencies. A theoretical model was developed for a single composite plate accounting for bending, membrane and shear motions in the displacement field. Rayleigh–Ritz method in conjunction with Hamilton principles was used to derive the equations of motion. Artificial springs were used to deal with arbitrary boundary conditions and in the present investigation emphasis was put on the free–free boundary conditions although the validation was extended and established for simply supported boundary conditions. The whole matrix obtained by minimizing the function of Hamilton exhibits a decoupling between the bending and the membrane motions. This property was used to determine the behavior of the two motions separately.

The model was first validated by comparing the first bending natural frequencies of a square aluminum plate with available data in the literature. Excellent agreement was found with a maximum discrepancy of 0.25%. The validation was then extended to the case of in-plane vibration. The upper limit of the discrepancy was found to be 0.02%. The validation was also established for simply supported boundary conditions for orthotropic plates by comparing results with existing data in the literature using Finite element codes. Results show same pattern of the first two natural frequencies when varying ply orientations.

The effect of the ply orientations on the bending fundamental frequency of a square composite plate was then studied. It was found that this frequency is symmetrical with respect to the 45° orientation. It decreases from 0° to 45° and increases from 45° to 90°.

Regarding the in-plane vibration, the simulation showed an inverse behavior for the first natural frequency of the membrane motion. It reaches a maximum for the 45° orientation and it is symmetrical with respect to this orientation. Simulations performed on the next seven natural frequencies showed that they all do not exhibit the same behavior and that special attention must be paid when developing tools for the design of composite plates.

The authors believe that the present analysis will be helpful when developing tools for designing composite materials since in-plane vibration is important in composite plates as reported in previous studies with regards to the dynamics of complex systems. The knowledge of the in-plane vibration can complement the one related to the bending vibration. This combined information can be used to tailor ply orientations to design composites for specific applications. The modeling proposed in the present paper is general as it includes a general modeling to deal with arbitrary conditions. In the present investigation emphasis is put on free–free boundary conditions. As highlighted in the present paper, the authors have validated the formulation for orthotropic plates under simply supported boundary conditions. Work is under investigation to explore the effect of combinations of boundary conditions with varying ply orientation.

Acknowledgments

The authors express their thanks to all the reviewers who provided critical comments and valuable suggestions. The first author would like to thank the upper management of Hawker Beechcraft Corporation for positive comments on the manuscript and for authorizing the publication of the paper.

Appendix. Definition of the parameters K_i and M_i [23, 24–27]

$$K_1 = \int\int_S \frac{\partial^2 \Psi_n(x_1)}{\partial x_1^2} \Psi_m(x_2) \frac{\partial^2 \Psi_p(x_1)}{\partial x_1^2} \Psi_q(x_2)\, \mathrm{d}S,$$

$$K_2 = \int\int_S \Psi_n(x_1) \frac{\partial^2 \Psi_m(x_2)}{\partial x_2^2} \Psi_p(x_1) \frac{\partial^2 \Psi_q(x_2)}{\partial x_2^2}\, \mathrm{d}S,$$

$$K_4 = \int\int_S \frac{\partial \Psi_n(x_1)}{\partial x_1}\frac{\partial \Psi_m(x_2)}{\partial x_2}\frac{\partial \Psi_p(x_1)}{\partial x_1}\frac{\partial \Psi_q(x_2)}{\partial x_2}\,\mathrm{d}S,$$

$$K_5 = \int\int_S \frac{\partial^2 \Psi_n(x_1)}{\partial x_1^2}\Psi_m(x_2)\frac{\partial \Psi_p(x_1)}{\partial x_1}\Psi_q(x_2)\,\mathrm{d}S,$$

$$K_6 = \int\int_S \Psi_n(x_1)\frac{\partial^2 \Psi_m(x_2)}{\partial x_2^2}\frac{\partial \Psi_p(x_1)}{\partial x_1}\Psi_q(x_2)\,\mathrm{d}S,$$

$$K_7 = \int\int_S \frac{\partial \Psi_n(x_1)}{\partial x_1}\frac{\partial \Psi_m(x_2)}{\partial x_2}\Psi_p(x_1)\frac{\partial \Psi_q(x_2)}{\partial x_2}\,\mathrm{d}S,$$

$$K_8 = \int\int_S \Psi_n(x_1)\frac{\partial^2 \Psi_m(x_2)}{\partial x_2^2}\Psi_p(x_1)\frac{\partial \Psi_q(x_2)}{\partial x_2}\,\mathrm{d}S,$$

$$K_9 = \int\int_S \frac{\partial^2 \Psi_n(x_1)}{\partial x_1^2}\Psi_m(x_2)\Psi_p(x_1)\frac{\partial \Psi_q(x_2)}{\partial x_2}\,\mathrm{d}S,$$

$$K_{10} = \int\int_S \frac{\partial \Psi_n(x_1)}{\partial x_1}\frac{\partial \Psi_m(x_2)}{\partial x_2}\frac{\partial \Psi_p(x_1)}{\partial x_1}\Psi_q(x_2)\,\mathrm{d}S,$$

$$K_{11} = M_1 = \int\int_S \frac{\partial \Psi_n(x_1)}{\partial x_1}\Psi_m(x_2)\frac{\partial \Psi_p(x_1)}{\partial x_1}\Psi_q(x_2)\,\mathrm{d}S,$$

$$K_{12} = M_2 = \int\int_S \Psi_n(x_1)\frac{\partial \Psi_m(x_2)}{\partial x_2}\Psi_p(x_1)\frac{\partial \Psi_q(x_2)}{\partial x_2}\,\mathrm{d}S,$$

$$K_{13} = \int\int_S \frac{\partial \Psi_n(x_1)}{\partial x_1}\Psi_m(x_2)\Psi_p(x_1)\frac{\partial \Psi_q(x_2)}{\partial x_2}\,\mathrm{d}S,$$

$$K_{14} = \int\int_S \Psi_n(x_1)\frac{\partial \Psi_m(x_2)}{\partial x_2}\frac{\partial \Psi_p(x_1)}{\partial x_1}\Psi_q(x_2)\,\mathrm{d}S,$$

$$K_{15} = M_3 = \int\int_S \Psi_n(x_1)\Psi_m(x_2)\Psi_p(x_1)\Psi_q(x_2)\,\mathrm{d}S,$$

$$K_{21} = \int\int_S \left[\frac{\partial^2 \Psi_n(x_1)}{\partial x_1^2}\Psi_m(x_2)\Psi_p(x_1)\frac{\partial^2 \Psi_q(x_2)}{\partial x_2} + \Psi_n(x_1)\frac{\partial^2 \Psi_m(x_2)}{\partial x_2^2}\frac{\partial^2 \Psi_p(x_1)}{\partial x_1^2}\Psi_q(x_2)\right]\mathrm{d}S,$$

$$K_{22} = \int\int_S \left[\frac{\partial^2 \Psi_n(x_1)}{\partial x_1^2}\Psi_m(x_2)\frac{\partial \Psi_p(x_1)}{\partial x_1}\frac{\partial \Psi_q(x_2)}{\partial x_2} + \frac{\partial \Psi_n(x_1)}{\partial x_1}\frac{\partial \Psi_m(x_2)}{\partial x_2}\frac{\partial^2 \Psi_p(x_1)}{\partial x_1^2}\Psi_q(x_2)\right]\mathrm{d}S,$$

$$K_{23} = \int\int_S \left[\Psi_n(x_1)\frac{\partial^2 \Psi_m(x_2)}{\partial x_2^2}\frac{\partial \Psi_p(x_1)}{\partial x_1}\frac{\partial \Psi_q(x_2)}{\partial x_2} + \frac{\partial \Psi_n(x_1)}{\partial x_1}\frac{\partial \Psi_m(x_2)}{\partial x_2}\Psi_p(x_1)\frac{\partial^2 \Psi_q(x_2)}{\partial x_2^2}\right]\mathrm{d}S,$$

$$K_{24} = \int\int_S \left[\frac{\partial \Psi_n(x_1)}{\partial x_1}\Psi_m(x_2)\Psi_p(x_1)\frac{\partial \Psi_q(x_2)}{\partial x_2} + \Psi_n(x_1)\frac{\partial \Psi_m(x_2)}{\partial x_2}\frac{\partial \Psi_p(x_1)}{\partial x_1}\Psi_q(x_2)\right]\mathrm{d}S,$$

$$K_{30} = M_4(p, q, n, m),$$

$$K_{31} = M_5(p, q, n, m).$$

References

[1] C.W. Bert, Optimal design of a composite-material plate to maximize its fundamental frequency, *Journal of Sound and Vibration* 50 (2) (1977) 229–237.
[2] C.W. Bert, Design of clamped composite-material plates to maximize fundamental frequency, *Transactions of the ASME, Journal of Mechanical Design* 100 (1978) 274–278.
[3] R. Woodcock, J. Nicolas, A generalized model for predicting the sound transmission properties of orthotropic plates with general boundary conditions, *Journal of the Acoustical Society of America* 97 (2) (1995) 1099–1112.
[4] D. Mohan, H.B. Kingsbury, Free vibrations of generally orthotropic plates, *Journal of the Acoustical Society of America* 50 (1, Part. II) (1971) 266–269.
[5] P.S. Nair, S. Durvasula, Vibration of generally orthotropic skew plates, *Journal of the Acoustical Society of America* 55 (5) (1974) 998–1002.
[6] S.K. Malhotra, N. Ganesan, M.A. Veluswami, Effect of fibre orientation and boundary conditions on the vibration behaviour of orthotropic square plates, *Composite Structures* 9 (1988) 247–255.
[7] D.J. Gorman, Accurate analytical type solutions for the free in-plane vibration of clamped and simply supported rectangular plates, *Journal of Sound and Vibration* 276 (2004) 311–333.
[8] D.J. Gorman, Free in-plane vibration analysis of rectangular plates by the method of superposition, *Journal of Sound and Vibration* 272 (2004) 831–851.
[9] J.N. Reddy, *Mechanics of Laminated Composite Plates—Theory and Analysis*, CRC Press, New York, 1997.
[10] R. Woodcock, Free vibration of advanced anisotropic multilayered composites with free–free boundary conditions, *Journal of Sound and Vibration* (2007), accepted for publication.
[11] A. Berry, J.-L. Guyader, J. Nicolas, A general formulation for the sound radiation from rectangular baffled plates with arbitrary boundary conditions, *Journal of the Acoustical Society of America* 88 (6) (1990) 2792–2802.
[12] P. Muthukumaran, R.B. Bhat, I. Stiharu, Boundary conditioning technique for structural tuning, *Journal of Sound and Vibration* 220 (5) (1999) 847–859.
[13] D.J. Gorman, A general solution for the free vibration of rectangular plates resting on uniform elastic edge supports, *Journal of Sound and Vibration* 139 (2) (1990) 325–335.
[14] D.J. Gorman, *Free Vibration Analysis of Rectangular Plates*, Elsevier North Holland, New York, 1982.
[15] N.S. Bardell, R.S. Langley, J.M. Dunsdon, On the free in-plane vibration of isotropic rectangular plates, *Journal of Sound and Vibration* 191 (3) (1996) 459–467.
[16] S.K. Malhotra, N. Ganesan, M.A. Veluswami, Effect of fibre orientation and boundary conditions on the vibration behaviour of orthotropic square plates, *Computers and Structures* 29 (5) (1988) 825–829.
[17] R. Woodcock, Modeling of Sound Transmission of Single-layer and Multi-layered Anisotropic Composite Structures with Arbitrary Boundary Conditions, PhD Thesis in French, Sherbrooke University, Sherbrooke, Québec, Canada, 1993.